Second-harmonic generation in optically trapped nonlinear particles with pulsed lasers

Malmqvist, Lennart; Hertz, H. M

Published in:
Applied Optics

DOI:
10.1364/AO.34.003392

1995

Second-harmonic generation in optically trapped nonlinear particles with pulsed lasers

L. Malmqvist and H. M. Hertz

Pulsed lasers are used for simultaneous single-beam three-dimensional optical trapping of and second-harmonic generation in 50–100-nm nonlinear particles. The emission power of the frequency-doubled light, the trapping stability, and the particle degradation are investigated for KTP and $LiNbO_3$ particles trapped by 25-kHz-repetition-rate *Q*-switched Nd:YAG and 76-MHz mode-locked Ti:sapphire lasers. Typically 1 pW–10 nW of frequency-doubled light is detected from stably trapped particles. The particles may be used as probes for nonintrusively scanned near-field optical microscopy.

Key words: Optical trapping, second-harmonic generation, microscopic particles.

1. Introduction

Single-beam optical trapping[1] of microscopic lithium niobate ($LiNbO_3$) particles with cw lasers results in the emission of frequency-doubled light from the particles.[2] This subwavelength visible light source is useful as a nonintrusive probe for scanning near-field optical microscopy.[3,4] However, the emitted power is limited because of the use of a cw trapping beam. In the present paper we increase the power by using *Q*-switched and mode-locked trapping lasers and investigate the stability, emission characteristics, and particle behavior of 50–100-nm potassium titanyl phosphate (KTP) and $LiNbO_3$ particles three-dimensionally trapped by such pulsed lasers.

The single-beam gradient-force optical trap provides an efficient method for nonintrusive manipulation and positioning of dielectric particles.[1] The trap consists of a cw laser beam focused with a high-N.A. microscope objective into, e.g., water containing small dielectric particles. The particles are trapped just below the focus as a result of the scattering and the gradient forces that are due to radiation pressure. With this trap, dielectric particles in the size range from tens of nanometers to tens of micrometers have been trapped. Furthermore, the trapping and manipulation of live viruses, cells, and subcellular organisms have been demonstrated,[5,6] yielding information on, e.g., cell motility,[7] making the trap an interesting tool for biology.

Recently, second-harmonic generation from micrometer-sized $LiNbO_3$ particles trapped by a cw Nd:YAG laser was observed.[2] Thus the laser simultaneously acts as the trapping beam and the fundamental beam for the second-harmonic generation. With the cw beam, the emitted frequency-doubled power is low, typically a fraction of a picowatt for sub-100-nm particles.[4] Because of the quadratic intensity dependence of the emitted power, it is favorable to use pulsed lasers to generate the frequency-doubled light, while still keeping the average power low to minimize heating. However, high-repetition-rate systems are necessary for stable trapping of submicrometer particles to prevent the escape of the particle from the trap between the pulses. For large objects, trapping by a scanning and a low-frequency chopped cw beam has been demonstrated.[8,9] In the present paper we discuss experiments with a 10–25-kHz-repetition-rate Nd:YAG laser as well as a 76-MHz Ti:sapphire laser. To our knowledge, this is the first investigation of simultaneous three-dimensional optical trapping and frequency doubling with pulsed lasers. In addition to the previously used material, $LiNbO_3$, we report simultaneous optical trapping and second-harmonic generation in KTP particles. This material has advantages compared with $LiNbO_3$, the most important being less variation in the emitted intensity from different particles.

Optically trapped nonlinear particles are useful as microscopic probes for nonintrusive near-field optical microscopy.[4] With a pulsed trapping beam the emitted frequency-doubled intensity could be increased to allow fluorescence studies, while still keeping the

The authors are with the Department of Physics, Lund Institute of Technology, P.O. Box 118, S-22100 Lund, Sweden.

Received 17 May 1994; revised manuscript received 13 December 1994.

0003-6935/95/183392-06$06.00/0.

average power of the trapping beam below the approximately 100-mW thermal-damage threshold of, e.g., biological objects.[10]

2. Experiments

The experimental arrangement for measurements with the Nd:YAG laser is shown in Fig. 1. The $\lambda = 1.06$ μm, 10–25-kHz acousto-optically *Q*-switched laser was linearly polarized. Depending on pump power and, thus, on laser power, the FWHM temporal pulse width varied from 320 to 950 ns for 25-kHz operation. The laser beam is focused into a water cell with a N.A. = 1.25 water immersion objective. The FWHM of the focal spot is approximately 450 nm.[4] The nonlinear particles are injected near the focus with a small syringe and are trapped just below the focus. The frequency-doubled light from the nonlinear crystals is collected with N.A. = 0.4 detection efficiency, which is taken into account in the comparison with the theoretical calculations of the frequency-doubled intensity in Section 3. The collected power is focused into a quartz optical fiber, and through interference ($\lambda = 532$ nm) and IR blocking filters (KG3) for spectral background reduction, the collected power is detected with a photomultiplier (Hamamatsu R1527) and a lock-in amplifier (EG&G 5209). We carefully checked that the strong IR beam was completely blocked and did not cause any spurious signal. The absolute collected power was determined from the measured current by the use of the manufacturers' data on the photomultiplier tube quantum efficiency and current amplification and the filter transmission given for the specific photomultiplier tube and filters used. The losses due to the coupling into the quartz fiber were measured in each experiment at the fundamental wavelength, and we compensated for them. Control measurements show no wavelength-dependent attenuation in the fiber. We compensated for the losses in the detection optics. Furthermore, for the theoretical calculations below, the absolute power of the trapping beam in the focal region must be determined. This was measured with the two-objective method described in Ref. 11. In the Ti:sapphire measurements described below, the same procedure for determining the absolute frequency-doubled emitted power and the trapping beam power was used, differing only in the use of a $\lambda = 397$ nm interference filter and a BG 38 IR blocking filter.

We produced both the KTP and the $LiNbO_3$ particles by grinding a piece of crystal in a mortar and mixing the powder with distilled water. After a few days of sedimentation, the top layer of the particle–water mixture is used for injection in the trap. The size range of the particles was determined by the use of scanning electron microscopy. The particles feature sharp edges and irregular shapes. The large majority of the KTP particles were in the 50–150-nm-diameter range. For $LiNbO_3$ the corresponding range was 50–100 nm. The size of the particle that is actually trapped was determined by measurement of the intensity of the scattered light from the trapping beam with an IR camera at right angles to the beam. This intensity is compared with the intensity scattered by 75-nm-diameter SiO_2 particles ($n \approx 1.5$) trapped in the same experimental arrangement. Assuming Rayleigh scattering and correcting for the different refractive indices of KTP ($n = 1.8$) and $LiNbO_3$ ($n \approx 2.2$), the diameter of the nonlinear particle in the trap may be determined.[12]

Figure 2 depicts the average power of the detected frequency-doubled light ($\lambda = 532$ nm) as a function of the average fundamental power in the focus for three KTP particles with diameters of 60, 95, and 115 nm. The curves have been normalized to 80-nm-diameter particles, assuming that the emitted frequency-doubled power is proportional to the radius to the 6th power (cf. Section 3). The normalization was performed to show the fluctuations in the emitted power for particles of the same size but with different orientation in the trap (cf. Section 3). For an 80-nm

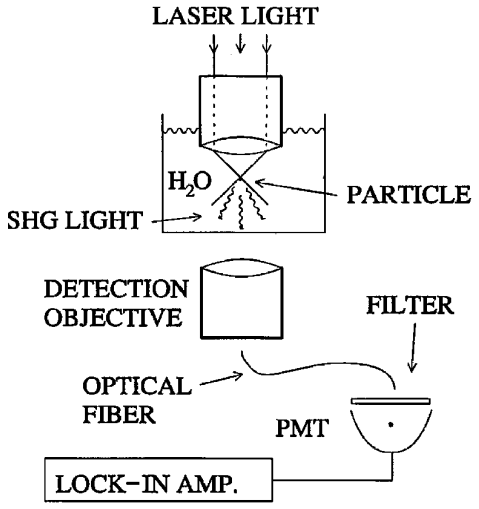

Fig. 1. Experimental arrangement for simultaneous optical trapping and second-harmonic generation (SHG). PMT, photomultiplier tube.

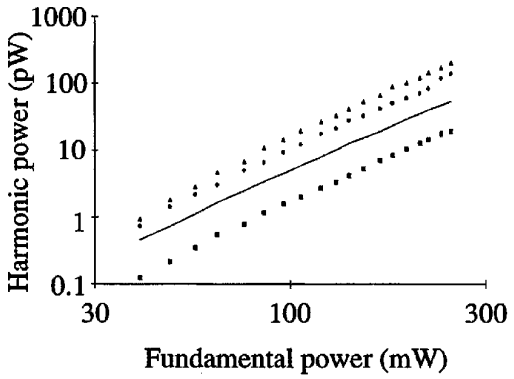

Fig. 2. Detected frequency-doubled power ($\lambda = 532$ nm) as a function of fundamental trapping power ($\lambda = 1.06$ μm) for three KTP particles trapped by a 25-kHz *Q*-switched Nd:YAG laser. The data have been normalized to 80-nm-diameter particles, and the original particles were 60 (▲), 95 (■), and 115 (●) nm. The solid curve represents the theoretically calculated power.

KTP particle, 100 and 250 mW of average trapping power produce up to 20 and 200 pW of detected frequency-doubled light, respectively. Using N.A. = 1 detection would increase the detected light to approximately 0.1 and 1 nW, respectively. For comparison, a theoretical curve (solid curve) based on the calculations in Section 3 is included in Fig. 2. Time-resolved measurements show that the emitted power follows the incident power temporally.

Similar experiments with $LiNbO_3$ particles yield up to 25 pW for 100-mW trapping power. For this material, however, the variation in emitted power between different particles is approximately 3 times larger than for the KTP, which is probably due to the larger spread in the magnitude of the nonlinear tensor components in $LiNbO_3$ compared with KTP. This is in fair agreement with theory and is further discussed in Section 3.

In the experiments discussed above, the repetition rate of the laser was 25 kHz. Lowering the repetition rate to 10 kHz, while keeping the average power constant, increases the emitted power because of shortening of the pulses. However, for repetition rates below 10 kHz, trapping became unstable and was hard to achieve at high trapping power (>200 mW). The instability for low repetition rates is probably due to an increased probability of the particle diffusing out of the trap between the pulses. When high trapping power is used, the slight heating of the bottom of the water cell accelerates other particles in the water cell toward the focus, which may cause the loss of the trapped particle.

To obtain higher frequency-doubled power, similar experiments were performed with a Ti:sapphire laser that generated 100-fs pulses with a 76-MHz repetition rate at $\lambda = 795$ nm. The high repetition rate eliminates diffusion between the pulses. The peak power from this laser was of the order of 1000 W compared with the 10 W from the *Q*-switched Nd:YAG laser. The FWHM of the focus was approximately 350 nm. Figure 3 depicts the average power of the detected frequency-doubled light as a function of the average fundamental power in the focus for three KTP particles with diameters of 70, 70, and 85 nm. As above, the curves have been normalized to 80-nm-diameter particles. The detected frequency-doubled power from an 80-nm particle reaches 4 nW, with a trapping power of 20 mW. Attempts to trap $LiNbO_3$ with the Ti:sapphire laser were unsuccessful.

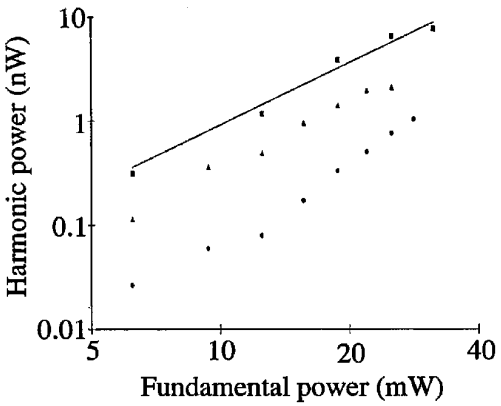

Fig. 3. Emitted frequency-doubled power ($\lambda = 397$ nm) as a function of incident power ($\lambda = 795$ nm) for three KTP particles trapped by a 76-MHz mode-locked Ti:sapphire laser. The data have been normalized to 80-nm-diameter particles, and the original particles were 70 (▲), 70 (■), and 85 (●) nm. The solid curve represents the theoretically calculated power.

However, when the femtosecond laser is used, the power of the frequency-doubled light decreases with time because of degradation of the particles. This behavior is similar to bleaching of fluorescent probes. The second-harmonic power was halved in 2 min. To slow down the degradation of the particles, we increased the pulse length to 800 fs by introducing dispersion in the beam with two prisms. This increased the lifetime of the particles to approximately 5 min before the intensity was halved. The output power as a function of time is shown in Fig. 4. In Fig. 4 30-mW input power was used. For comparison, the emitted power from KTP as a function of time when 50-mW Nd:YAG laser power is used is also plotted in Fig. 4. It is evident that particle degradation is not a problem with this laser.

The cause of the degradation is not clear. Simultaneous measurements of the decreasing frequency-doubled emission and the scattered IR light indicate that the particle size is constant. Thus the particle is not physically damaged, and the decrease in second-harmonic intensity may be due to altered nonlinear properties of the material.

3. Theory and Discussion

In this section we discuss the stability and the motion of particles trapped by a pulsed laser. Furthermore, the experimentally measured frequency-doubled emitted power is compared with theoretical calculations. In both cases it is assumed that the particle diameter is much less than the wavelength, i.e., that Rayleigh-scattering theory is valid. This is in fair agreement with the particles used in the experiments discussed above.[13]

For cw-laser optical trapping, the stability is determined by the scattering and the gradient forces that are due to radiation pressure and the Brownian motion of the particle in the trap. When Rayleigh

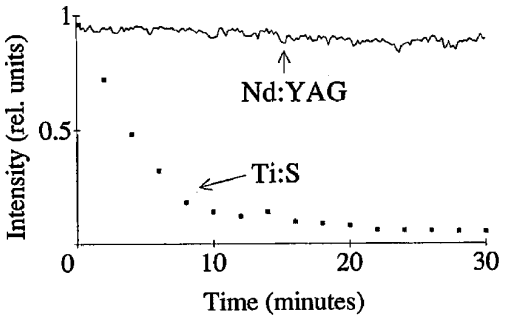

Fig. 4. Stability of the frequency-doubled emission from KTP particles as a function of the time when a *Q*-switched Nd:YAG laser and a mode-locked Ti:sapphire laser are used.

particles are assumed, the forces are easily calculated.[3,4] With a cw 100-mW, $\lambda = 1.06$ μm trapping beam focused to FWHM = 450 nm, the force constant in the radial direction (k_r) in the harmonic oscillator is typically ~5 pn/μm for an 80-nm-diameter particle with $n \approx 2$. Calculations of the particle diffusion (Brownian motion) in the trap may be performed if it is assumed that the trap is a harmonic potential well.[3] The root mean square (rms) displacement from the equilibrium position is[14]

$$\sqrt{\langle r^2 \rangle} = \left(\frac{kT}{k_r}\right)^{1/2}, \tag{1}$$

where k is Boltzmann's constant and T is the temperature. Typically the rms displacement is 25 nm. In the vertical z direction the rms displacement is typically twice this value because of the smaller intensity gradients. In a viscous liquid such as water, these values are reached after approximately a millisecond.[14] When pulsed lasers are used for the trapping, particle diffusion between the pulses has to be taken into account. The rms displacement in the absence of light forces may be written as[14]

$$\sqrt{\langle r^2 \rangle} = \left(\frac{kT}{3\pi a \eta}\, t\right)^{1/2}, \tag{2}$$

where a is the particle radius, η is the viscosity, and t is the time. For the above-mentioned particles, at room temperature the rms displacement is approximately 20 nm for $t = 40$ μs, corresponding to 25-kHz laser operation. Thus the rms displacement is small for the 25-kHz and higher repetition rates used in this paper. However, for lower repetition rates the probability of particle escape, i.e., that the particle diffuses outside the capture range of the trap between the pulses, becomes significant, which is in agreement with experiments.

The emitted frequency-doubled power was determined theoretically with the assumption that the nonlinear particle is a sphere. The nonlinear polarization $\mathbf{P}(2\omega) = 2\varepsilon_0 \mathbf{d} \mathbf{E}_1{}^2$ was calculated conventionally following Ref. 15. Here ε_0 is the vacuum permittivity, $\mathbf{d}$ is the nonlinear susceptibility tensor, and $\mathbf{E}_1$ are the electric-field components (as defined in Ref. 15) at the fundamental frequency inside the particle. The magnitude of the electric field inside the particle is assumed to be[12]

$$E_1 = \frac{3\varepsilon_2}{\varepsilon_1 + 2\varepsilon_2} E_2, \tag{3}$$

where E_2 is the fundamental electric field that is due to the trapping beam in the water and in absence of the particle and ε_1 and ε_2 are the linear permittivities of the particle and the water, respectively. The nonlinear susceptibility tensors and data are given in Refs. 15 and 16 for $LiNbO_3$ and KTP, respectively. Because of the small size of the particle, it may be regarded as a dipole source at the second-harmonic frequency, with dipole moment components of $(4/3)\pi a^3 P_i(2\omega)$, where $P_i(2\omega)$ are the elements of the nonlinear polarization ($i = x, y, z$). The total emitted power from a dipole is given by Ref. 17, resulting in

$$W_{\text{tot}} = \frac{64\pi^5 c a^6}{27\varepsilon_0 n_2{}^3 \lambda^4} \sum [P_i(2\omega)]^2, \tag{4}$$

where c is the speed of light, n_2 is the refractive index of water, and λ is the wavelength in the water.

The theoretically calculated second-harmonic power is compared with the experimentally measured data in Figs. 2 and 3, where it is included as a solid line. In Figs. 2 and 3 collection efficiency and the decrease of the temporal pulse width with increasing laser power (for the Nd:YAG laser) have been taken into account. The temporal laser-pulse profile was assumed to be Gaussian. Temporal broadening of the Ti:sapphire pulses because of dispersion in the microscope objective is assumed to be small. Measurements on similar objectives show a <10% increase in pulse width.[18] The calculations were performed for particles with their crystal axes aligned for maximum second-harmonic emission. The slopes of our experimental curves agree well with the expected quadratic intensity dependence.

For the Nd:YAG laser the highest experimentally measured data are approximately a factor of 2 larger than the theoretically calculated power, and for the Ti:sapphire laser the difference is negligible. This is well within the accuracy of the experiments and the theory. The error in the theoretical calculations is dominated by the uncertainty of the size of the particle. The diameter of the nominally 75-nm SiO_2 particles used for the size determination may vary within ±15 nm (2σ). Because of the a^6 dependence in Eq. (4), this corresponds to an error in the calculated frequency-doubled power of approximately a factor of 3. Other errors contribute with less than a factor of 2. These errors are due to limited accuracy in the determination of the focal-region trapping beam intensity and in the nonlinear susceptibilities, and, for the larger particles, a slight deviation from Rayleigh theory, resulting in an increased intensity in the forward direction. The experimentally determined second-harmonic powers are estimated to be correct within 50%. Here the major sources of error are due to limited accuracy in the current and the fiber loss measurements and in the photomultiplier sensitivity and gain.

Theoretically, the difference in emitted power between the least and the most favorable orientations of the KTP crystal particle in the trap is a factor of 40, because of the difference in the nonlinear susceptibility tensor elements. If the particle rotated in the trap the output power should be an average of all different crystal orientations, resulting in a negligible variation compared with that of a nonrotating particle. Experimentally, we observe a particle-to-particle variation as large as a factor of 10, indicating that the particle does not rotate in the trap. Further evi-

dence for nonrotation is provided in the next paragraph. Similar calculations for $LiNbO_3$ results in a difference in the emitted second-harmonic power of a factor of 75, because of the larger difference in its nonlinear tensor components. Experimentally, the observed variation was a factor of 30. The lower particle-to-particle variations in the emitted power of KTP are advantageous when used as a microscopic light source. The difference between the experimentally and the theoretically determined particle-to-particle variations is probably due to the low probability of trapping a particle in an orientation that produces either very low or very high frequency-doubled power.

Because of the coupling between the elements in the nonlinear susceptibility tensor, the polarization of the frequency-doubled light may be different than the linearly polarized trapping beam. For a rotating particle, the polarization of the emitted light should change with time. Experimentally, the second-harmonic light was found to be linearly polarized. This provides further evidence that the particle is not rotating in the trap. The direction of the linear polarization differed up to 50° between different particles. The crystal orientation in the trap determines the polarization direction of the emitted light through the nonlinear susceptibility tensor.

It is interesting to note that second-harmonic generation in both the KTP and the $LiNbO_3$ particles functions well even after weeks in the water mixture. This is in contrast to GaAs, which would be an attractive material with its high nonlinear optical tensor components. After a short time in water, the GaAs particles cannot be trapped. One suggestion is that absorption of the particles increases because of diffusion of oxygen into dislocations introduced when the crystal is ground.[19]

This paper was initially motivated by our interest in using optically trapped particles as subwavelength light sources for nonintrusive scanning near-field optical microscopy. Such a source would be advantageous for high-resolution studies of, e.g., biological objects with intervening membranes, which prohibit the use of conventional mechanically positioned probes. Fluorescence studies require approximately a nanowatt of power,[20] while still keeping the average trapping power below the approximately 100-mW biological damage threshold.[10] The current experiments show that this requirement is met by the Ti:sapphire experiments, albeit only for a limited time, because of the degradation of the particles. However, from damage studies on rat liver cells[21] we estimate that the Ti:sapphire intensity should be reduced to approximately 5 mW so as not to induce apparent damage. Still, when N.A. = 1 detection is used, the collected power would approach a nanowatt. The longer pulses of the *Q*-switched Nd:YAG laser are in this respect advantageous, allowing an average trapping power of 100 mW before biological damage occurs. As mentioned above, this results in a detected power of approximately 0.1 nW when N.A. = 1 detection is used.

4. Conclusions

We have investigated pulsed lasers for simultaneous trapping of and optical frequency doubling in nonlinear particles. The emitted second-harmonic power was found to be quadratically dependent on the input power. Typically power of a few nanowatts was emitted within the N.A. = 0.4 detection cone from the Ti:sapphire laser, and the *Q*-switched Nd:YAG produced 0.01–0.2 nW. Because of the degradation of particles and the damage to biological samples in the Ti:sapphire experiments, the Nd:YAG laser currently seems more appropriate for nonintrusively scanning near-field optical microscopy. However, the emitted power is somewhat too low for fluorescence studies. Future experiments will focus on increasing the power by investigation of materials that exhibit very high second-harmonic conversion efficiency, such as synthetic crystals.[22] Because phase matching is not an issue in this application, many crystals that are not applicable to conventional optical second-harmonic generation may prove useful. Thus the require-ments for the material are relaxed, and water-insoluble crystals that have very high second-harmonic coefficients should be interesting. Alternatively, high-repetition-rate lasers with peak powers of 50–100 W may be useful, increasing the emitted power to a few nanowatts without causing particle degradation.

The support of and discussions with Fredrik Laurell, Kristina Georgsson, Bo Nilsson, Anders Persson, Ingrid Rokahr, and Lars Rymell are gratefully acknowledged. This work was supported by the Swedish Natural Science Research Council, the Swedish Board for Technical and Industrial Development, the Carl Trygger Foundation, and the Crafoord Foundation.

References

1. A. Ashkin, J. M. Dziedzic, J. E. Bjorkholm, and S. Chu, "Observation of single-beam gradient force optical trap for dielectric particles," Opt. Lett. **11,** 288–290 (1986).
2. S. Sato and H. Inaba, "Observation of second harmonic generation from optically trapped microscopic $LiNbO_3$ particle using Nd:YAG laser," Electron. Lett. **28,** 286–287 (1992).
3. L. Malmqvist and H. M. Hertz, "Trapped particle optical microscopy," Opt. Commun. **94,** 19–24 (1992).
4. L. Malmqvist and H. M. Hertz, "Two-color trapped particle optical microscopy," Opt. Lett. **19,** 853–855 (1994).
5. A. Ashkin and J. M. Dziedzic, "Optical trapping and manipulation of viruses and bacteria," Science **235,** 1517–1520 (1987).
6. W. H. Wright, G. J. Sonek, Y. Tadir, and M. W. Bems, "Laser trapping in cell biology," IEEE J. Quantum Electron. **26,** 2148–2157 (1990).
7. A. Ashkin, K. Schütze, J. M. Dziedzic, U. Euteneuer, and M. Schliwa, "Force generation of organelle transport measured *in vivo* by an infrared laser trap," Nature **348,** 346–348 (1990).
8. K. Sasaki, M. Koshioka, H. Misawa, N. Kitamura, and H. Masuhara, "Laser-scanning micromanipulation and spatial patterning of fine particles," Jpn. J. Appl. Phys. **30,** L907–L909 (1991).

9. K. Visscher, G. J. Brakenhoff, and J. J. Krol, "Micromanipulation by 'multiple' optical traps created by a single fast scanning trap integrated with the bilateral confocal scanning laser microscope," Cytometry **14,** 105–114 (1993).
10. S. M. Block, "Optical tweezers: a new tool for biophysics," in *Noninvasive Techniques in Cell Biology*, J. K. Foskett and S. Grinstein, eds. (Wiley, New York, 1990), pp. 375–402.
11. H. Misawa, M. Koshioka, K. Sasaki, N. Kitamura, and H. Masuhara, "Three-dimensional optical trapping and laser ablation of a single polymer latex particle in water," J. Appl. Phys. **70,** 3829–3836 (1991).
12. M. Kerker, *The Scattering of Light* (Academic, New York, 1969), Chap. 3.
13. W. Heller, "Theoretical investigations on the light scattering of spheres. XVI. Range of practical validity of the Rayleigh theory," J. Chem. Phys. **42,** 1609–1615 (1965).
14. S. Chandrasekhar, "Stochastic problems in physics and astronomy," Rev. Mod. Phys. **15,** 1–89 (1943).
15. R. W. Boyd, *Nonlinear Optics* (Academic, San Diego, Calif., 1992), pp. 39 and 432.
16. H. Vanherzeele and J. D. Bierlein, "Magnitude of the nonlinear-optical coefficients of $KTiOPO_4$." Opt. Lett. **17,** 982–984 (1992).
17. P. Lorrain and D. Corson, *Electromagnetic Fields and Waves*, 2nd ed. (Freeman, New York, 1970), p. 605.
18. S. Hell, Centre for Biotechnology, P.O. Box 123, Turku, Finland FIN-20521 (personal communication, 1994).
19. W. Seiffert, Department of Physics, Lund Institute of Technology, P.O. Box 118, Lund, Sweden S-22100 (personal communication, 1994).
20. J. K. Trautman, E. Betzig, J. S. Wiener, D. J. DiGiovanni, T. D. Harris, F. Hellman, and E. M. Gyorgy, "Image contrast in near-field optics," J. Appl. Phys. **71,** 4659–4663 (1992).
21. S. Andersson-Engels, I. Rokahr, and J. Carlsson, "Time- and wavelength-resolved spectroscopy in two-photon excited fluorescence microscopy," J. Microsc. (Oxford) **176** 195–203 (1994); I. Rokahr, Department of Physics, Lund Institute of Technology, P.O. Box 118, Lund, Sweden S-22100 (personal communication, 1994).
22. D. S. Chemla and J. Zyss, eds., *Nonlinear Optical Properties of Organic Molecules and Crystals* (Academic, New York, 1987).